Formation of oxide nanoclusters in nanostructured ferritic alloys during anisothermal heat treatment

C. Hin[1,2], B.D. Wirth[2], J.B. Neaton[3]

[1]Department of Materials Sciences and Engineering, Massachusetts Institute of Technology, Cambridge, MA 02139-4307, USA

[2]Department of Nuclear Engineering, University of California, Berkeley, CA 94720-1730, USA

[3]Molecular Foundry, Lawrence Berkeley National Laboratory, University of California, Berkeley, CA 94720-1730, USA

1. Introduction

Predicting and improving the performance of fission and fusion reactor materials is challenging, especially towards the higher operating temperature goals of fusion and Generation IV fission reactor systems. Advanced engineering alloys require achieving a balance of strength and fracture/creep resistance in an extremely fine dispersion. Prior works on this topic [1] show that a high-number density of nanoscale Y-Ti-O clusters can improve creep resistance. It is also believed that the Y-Ti-O clusters, in addition to impeding dislocations and reducing grain-boundary mobility, act as traps for insoluble helium that would be generated in fusion reactor structural components. However, many questions exist related to the formation, structure and thermal stability of these Y-Ti-O nanoparticles that affect the optimal processing method and their performance in extreme environments. For example, it is necessary to understand their kinetic pathway of precipitation during an anisothermal heat treatment in order to develop improved processing methods and fully understand their atomic-scale structure and composition. Kinetic Monte Carlo (KMC) techniques provide the ability to understand the kinetic paths controlling the precipitation of nanoclusters at the atomistic scale.

In this study, we provide insight into how oxides nanoclusters form in Fe-Ti-O and Fe-Y-O ternary alloys, shedding light on the complex kinetic pathway to precipitation in Fe-Y-Ti-O quaternary alloys. The kinetic pathway to precipitation in Fe-Y-O alloys has recently been studied extensively both experimentally [1] and computationally [2,3]. However, precipitation in Fe-Ti-O alloys has been poorly studied to this point.

After mechanical alloying, Y_2O_3 in the as-milled powders has not been detected by SANS or X ray measurement. This suggests that Y_2O_3 dissolves into yttrium and oxygen to re-precipitates with titanium to form Y-Ti-O nanoclusters during the thermomechanical heat treatment [1,4]. After thermo-mechanical treatments, small-angle neutron scattering studies reveal the presence of (i) Y_2O_3 nanoclusters with a c-type cubic crystal structure typical of the rare-earth oxides and bulk lattice parameter of 1.0604 nm [5]; and (ii) TiO_2 nanoclusters with a rutile structure and bulk lattice parameters equal to 0.4582 nm in <001> and <010> directions, and 0.2953 nm in the <100> direction [6], (iii) Ti_2O_3 nanoclusters with a rhombohedral structure (corundum, with a lattice parameters at room temperature equal to a=0.515 nm and b=1.362 nm [7]), as well as the existence of $Y_2Ti_2O_7$ and Y_2TiO_5 [1]. The lattice parameters of these different phases are large compared to ferrite. A loss of coherency is then expected during the anisothermal heat treatment. However, since the dimension of the precipitates is on the order of nanometers, we assume that they retain coherency with the matrix. This assumption can neither be confirmed nor invalidated because their small size is beyond the limits of characterization techniques. This makes describing the kinetic pathways of precipitation extremely challenging. Numerical models provide an alternative means for understanding nucleation.

2. Numerical method

2.1. Rigid lattice Approximation

The rigid lattice model and the assumptions used in this study have been fully explained in [2]. The alloy configuration is described on a simple cubic lattice (lattice parameter $a_{Fe}/2$) which can support both the body-centered cubic (BCC) structure of the α-Fe (including the octahedral sites of interstitial oxygen) as well as the Y_2O_3 and Ti_2O_3 structure. Note that because of this rigid lattice approximation, the TiO_2 structure cannot be reproduced.

2.2. Atomistic kinetic model

In the KMC model extensively developed in [2], variations in vacancy are described by a vacancy source and sink which naturally drives the vacancy concentration toward its equilibrium value. Whatever the temperature during the anisothermal heat treatment, the vacancy diffusion is then well reproduced. Thus, realistic mechanisms by vacancy or interstitial jumps are considered for diffusion of Fe, Ti and Y atoms located on substitutional sites of the BCC rigid lattice, and O atoms located in the interstitials.

For the purpose of conciseness, the details of the determination of parameters are explained in *Reference* [2].

3. Monte Carlo results

In the simulation results presented in **Figures 1**, the compositions and temperatures correspond to two-phase equilibrium states either between α-Fe and Y_2O_3 or α-Fe and Ti_2O_3. In order to compare the kinetic path of precipitation of Y_2O_3 and Ti_2O_3 in ferrite during a temperature ramp, simulations at relative high supersaturations (Fe-0.25 at.%Y-0.37 at.%O and Fe-0.25

at.%Ti-0.37 at.%O) have been performed during an anisothermal heat treatments starting from 600 K up to 1125 K with a ramp rate equal to 20 K/min. The anisothermal heat treatment begins for all the simulations at 600 K. Bellow this temperature, the diffusion coefficients of the different species are too small to observe an influence on the precipitation kinetics.

In each simulation, a vacancy source/sink ensures that the equilibrium value for vacancy concentrations is maintained along anisothermal heat treatments. The simulation boxes are comprised of 100×100×100 body centred cubic cells with full periodic boundary conditions. Even though the path of precipitation is practically the same (i.e. formation of a Fe_2O_3 metastable phases followed by the formation of the stable phases (Y_2O_3 of Ti_2O_3)), the kinetic is not the same, notably at the end of the temperature ramp, when the plateau is reached. For the Fe-Y-O ternary alloy, the system remains with 4.2×10^{24} m^{-3} $Fe_XY_{2-X}O_3$ (with X≈ 0.5) precipitates containing 15 atoms per precipitate (≈ 0.50 nm), while for the Fe-Ti-O ternary alloy, the system remains with 5.2×10^{23} m^{-3} $Fe_XTi_{2-X}O_3$ (with X≈ 1.2) precipitates containing 100 atoms per precipitate (≈ 1.2 nm). In the first case, at the end of the temperature ramp, the system has just reached the coarsening type reaction of the $Fe_XY_{2-X}O_3$ precipitates, while for the second case, it is almost the end of the coarsening type reaction of the $Fe_XTi_{2-X}O_3$ precipitates. Hence, 200 precipitates remain in the simulation box for the Fe-Y-O ternary alloy, while only 7 precipitates remain for the Fe-Ti-O system. This substantial difference is ascribed to the difference of diffusion coefficients between Y and Ti atoms. The Ti diffusion coefficient is about 10^5 times faster than the Y diffusion coefficient, whatever the temperature during the anisothermal heat treatment. That means that the whole kinetic path of precipitation for the Fe-Ti-O ternary alloy takes place during the temperature ramp.

Similar results are experimentally found in *References* [8-12]. This study concerns the MA957 alloy. Results reveal that the small precipitates are those principally composed of yttrium and oxygen and the large precipitates are those principally composed of titanium and oxygen. This result is probably also a consequence of the dramatically different diffusion rates of Y and Ti atoms.

We have also performed simulations for lower supersaturations for the Fe-Ti-O system. We conclude that the lower the supersaturation, the more the effect of the temperature ramp on the kinetic path.

4. Conclusion

To conclude, it seems to be important to choose an appropriate alloy composition and anisothermal heat treatment in order to better control the formation of these nanoparticles and therefore, the macroscopic properties, such as the creep resistance.

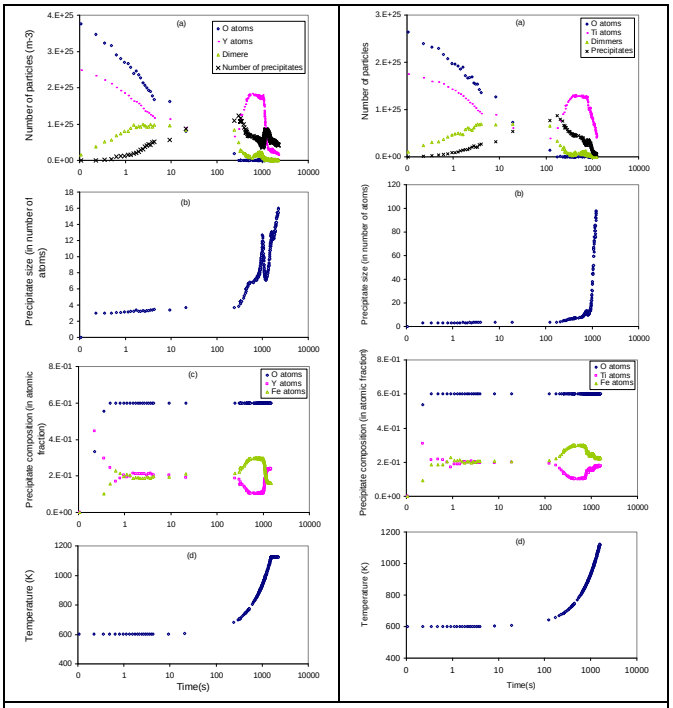

Figure 1: Monte Carlo simulation of homogeneous precipitation in Fe-0.25 at.%Y-0.37 at.%O and Fe-0.25 at.%Ti-0.37 at.%O. The temperature ramp rate is equal to 20 K/min, up to a maximum temperature of 1125 K. The simulation box is comprised of 100 × 100 × 100 BCC cells. Evolution of: (a) number of particles (m^{-3}), (b) precipitate size (in number of atoms), (c) precipitate composition (in atomic fraction), (d) Evolution of temperature as a function of time.

Acknowledgements. The authors gratefully acknowledge the financial support of the National Science Foundation under contract NSF DMR 0548259 and the Department of Energy, Office of Fusion Energy Sciences under grant DE-FG02-04GR54750. Portions of this work were performed at the Molecular Foundry, Lawrence Berkeley National Laboratory, which is supported by the Office of Science, Office of Basic Energy Sciences, of the U. S. Department of Energy under Contract No. DE-AC02-05CH11231.

References

[1] Alinger M. Ph. D. Thesis, University of Santa Barbara, 2004 and reference stherein.
[2] Hin C., Wirth B.D., J. Nuc. Mat. 402(1) (2010) 30.
[3] Hin C., Wirth B.D., Neaton J.B., Phys. Rev. B 80 (2009) 134118.
[4] M.J. Alinger, G.R. Odette and D.T. Hoelzer, J. Nuc. Mat. 329-333 (2004) 382-386.
[5] O'Connor B.H., Valentine T.M., Acta Cryst. B 25 (1969) 2140.
[6] Diebold U., Surface Science Reports 48 (2003) 53.
[7] Capponi J.J., Marezio M., Dumas J., Schlenker S., Solid State Communications 20 (1976) 893.
[8] Hamilton ML, Gelles DS, Lobsinger RJ, Johnson GD, Brown WF, et al. 2000. Fabrication technological developement of the oxide dispersion strengthened alloy MA 957 for fast rectr applications. PNL-13168, Richland, WA: Pac. Northwest Lab.
[9] S. Ukai, Okuda T, Fujiwara M, Kobayashi T, Mizuta S, Nakashima H, J. Nucl. Sci. Techno. 39 (2002) 872:879.
[10] Yamashita S, Akasaka N, Ukai S, Ohnuki S, J. Nuc. Mat. 367-370 (2007) 202-207.
[11] Kishimoto H, Alinger MJ, Odette GR, Yamamoto T, J. Nuc. Mat. 329-333 (2004) 369-71.
[12] Miao P, Odette GR, Yamamoto T, Alinger MJ, Klingensmith D, J. Nuc. Mat. 329-333 (2004) 369-71.